

Supporting Information

MOF-derived Fe,Co@N-C Bifunctional Oxygen Electrocatalysts for Zn-air Batteries

Xinde Duan,^a Shuangshuang Ren,^a Na Pan,^b Mingdao Zhang^{b*} and Hegen Zheng^{a*}

^a*State Key Laboratory of Coordination Chemistry, School of Chemistry and Chemical Engineering, Collaborative Innovation Center of Advanced Microstructures, Nanjing University, Nanjing 210023, P. R. China.*

^b*School of Environmental Science and Engineering, Nanjing University of Information Science & Technology, Jiangsu Key Laboratory of Atmospheric Environment Monitoring and Pollution Control, Collaborative Innovation Center of Atmospheric Environment and Equipment Technology, Nanjing 210044, P. R. China.*

**Corresponding authors*

E-mail: zhenghg@nju.edu.cn; matchlessjimmy@163.com

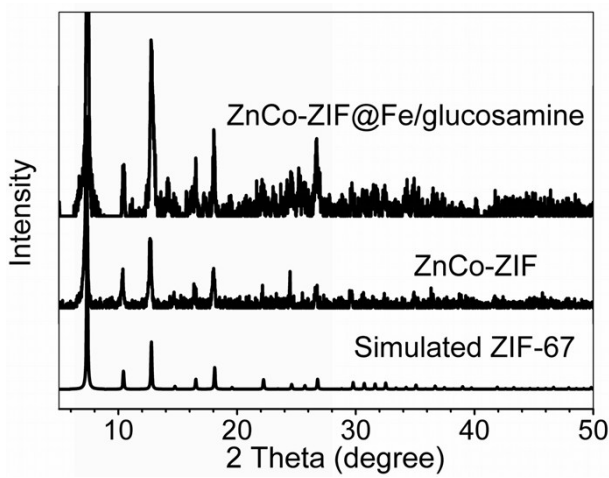


Fig. S1 PXRD patterns of ZnCo-ZIF@Fe/glucosamine and ZnCo-ZIF.

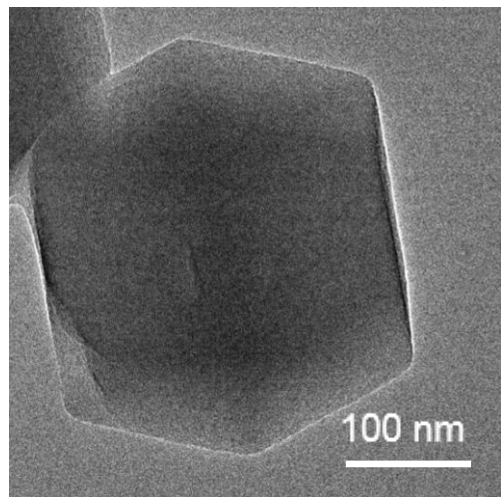


Fig. S2 SEM image of ZnCo-ZIF.

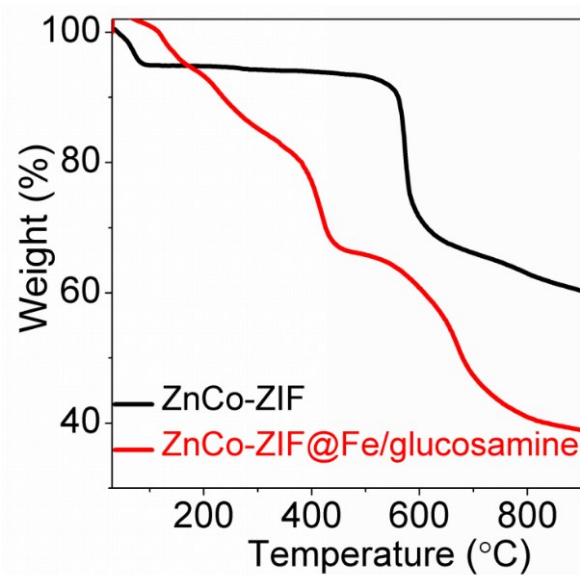


Fig. S3 Thermogravimetric plots of ZnCo-ZIF and ZnCo-ZIF@Fe/glucosamine under N_2 from 25 to 900 $^{\circ}\text{C}$ with a heating rate of $10 \text{ }^{\circ}\text{C min}^{-1}$.

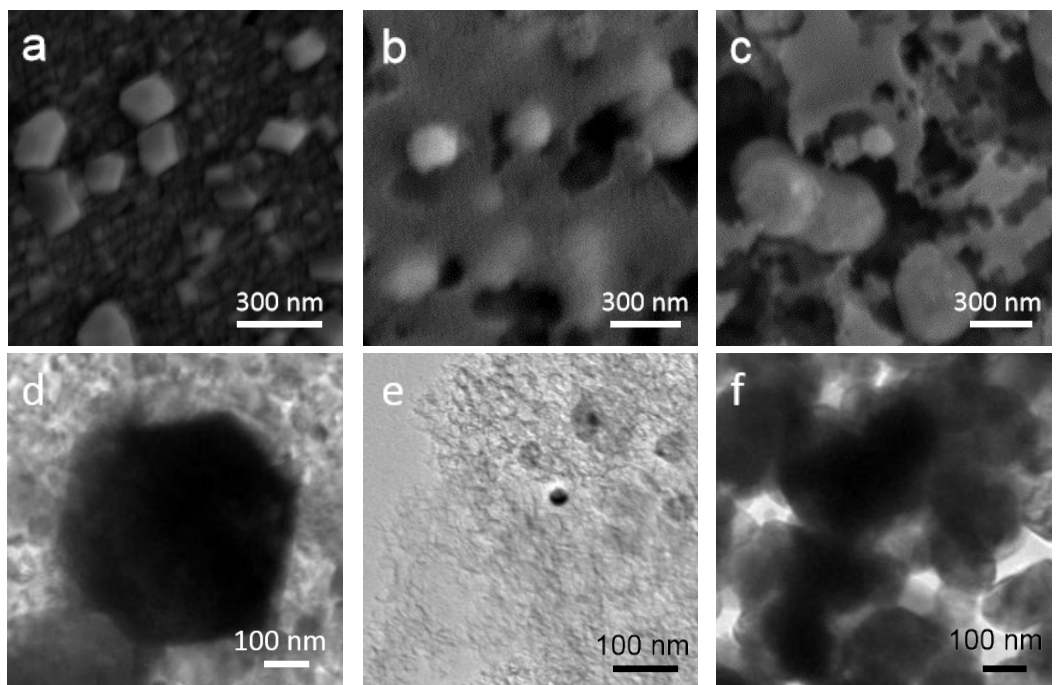


Fig. S4 SEM and TEM images of FeCo-N-C-600 (a, d), FeCo-N-C-700 (b, e), and FeCo-N-C-800 (c, f).

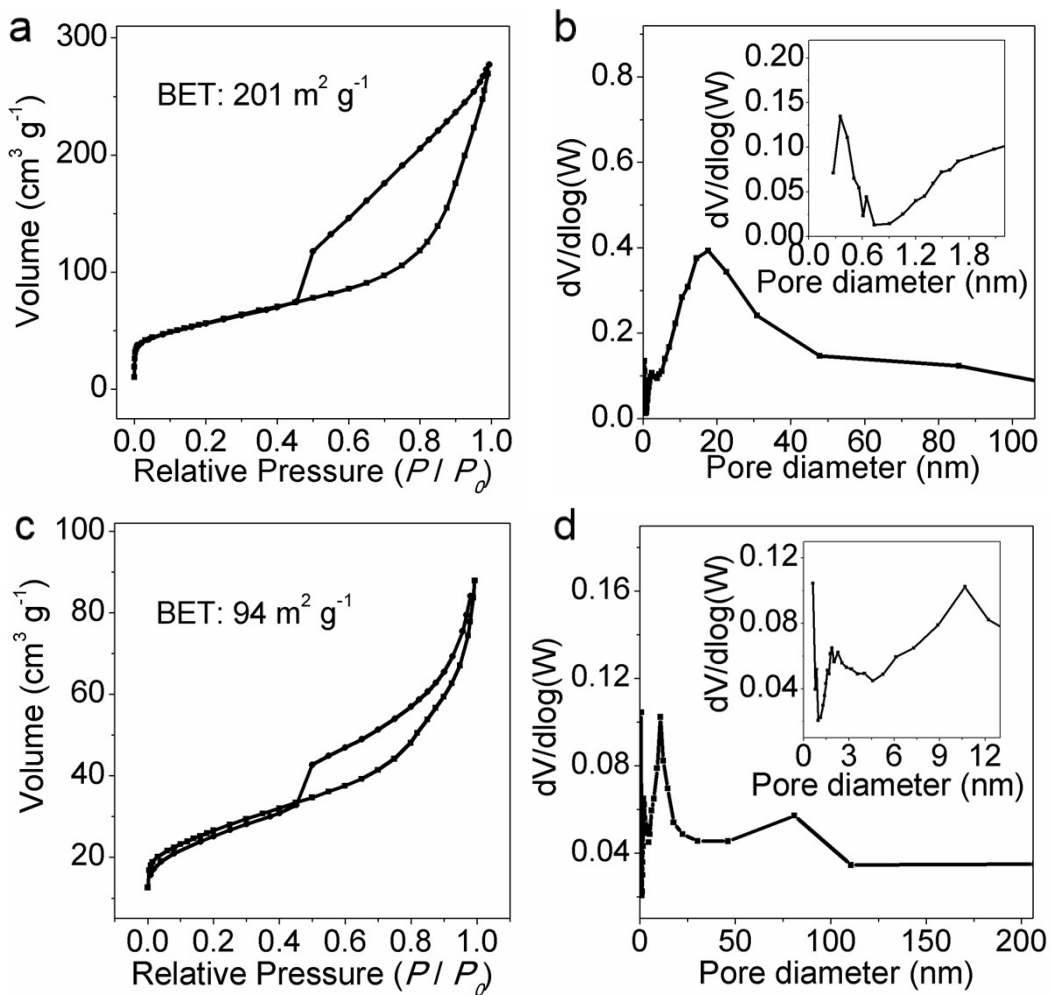


Fig. S5 N_2 adsorption/desorption isotherms and pore size distribution plots of FeCo-N-C-600 (a, b) and FeCo-N-C-800 (c, d).

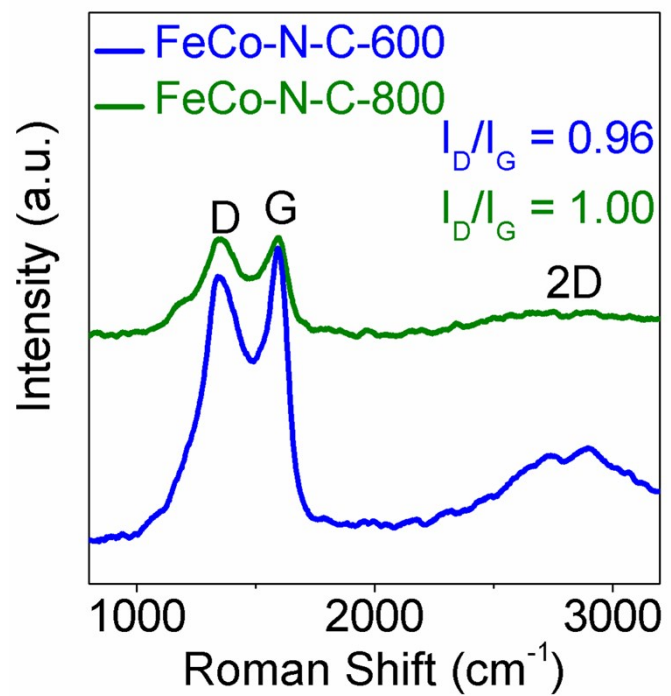


Fig. S6 Roman spectra of FeCo-N-C-600 and FeCo-N-C-800.

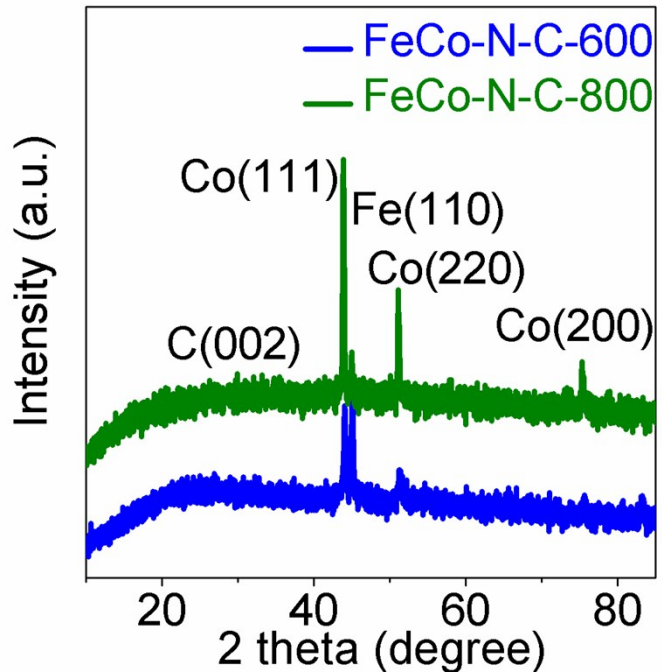


Fig. S7 PXRD patterns of FeCo-N-C-600 and FeCo-N-C-800.

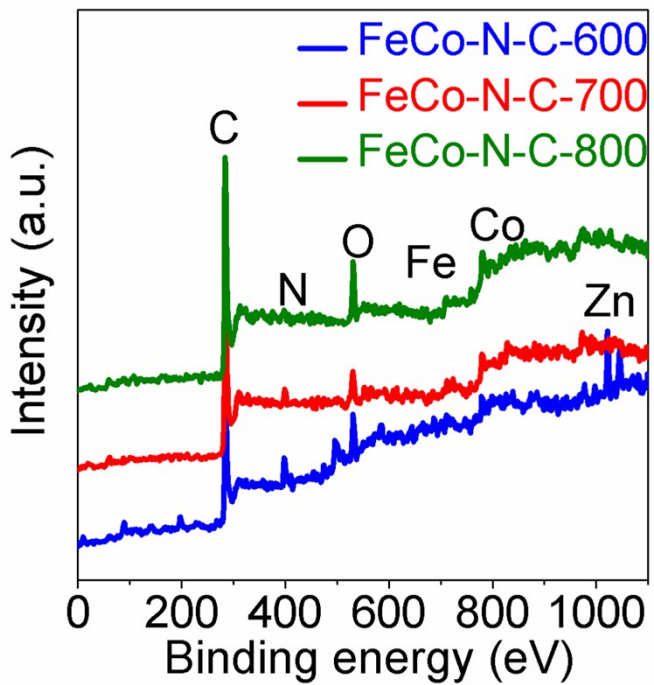


Fig. S8 XPS spectra of different catalysts.

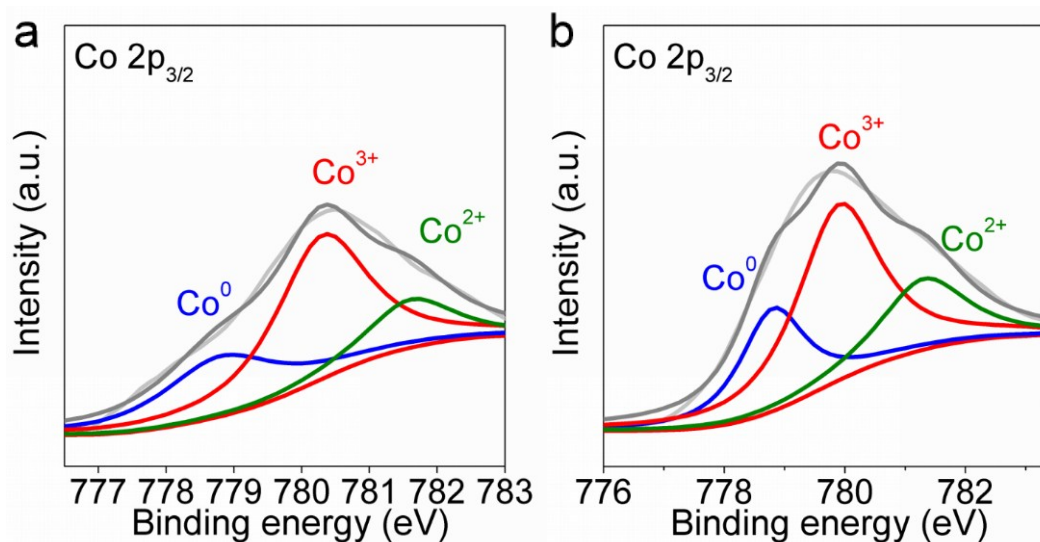


Fig. S9 The high resolution Co 2p XPS spectra of FeCo-N-C-600 (a) and FeCo-N-C-800 (b).

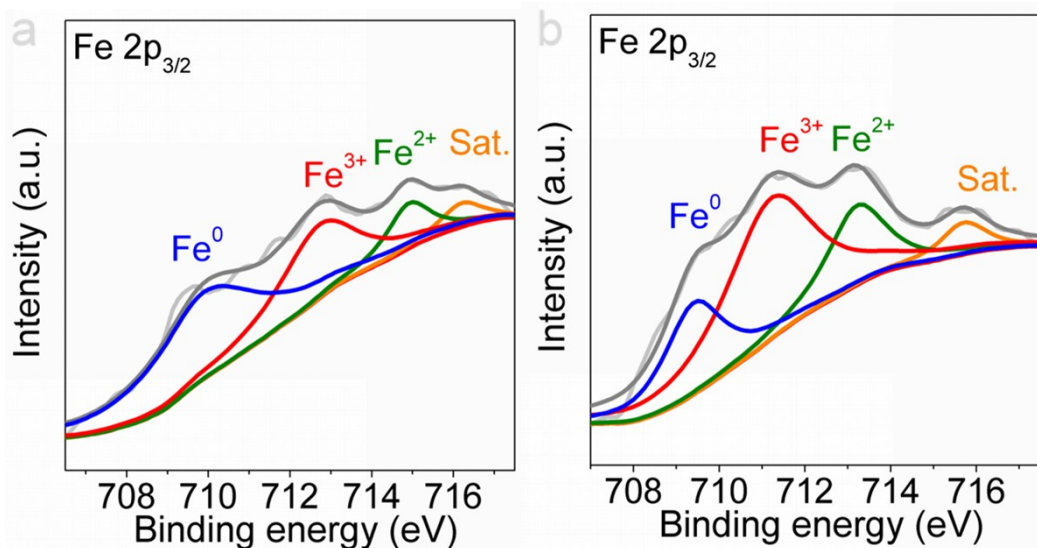


Fig. S10 The high resolution Fe 2p XPS spectra of FeCo-N-C-600 (a) and FeCo-N-C-800 (b).

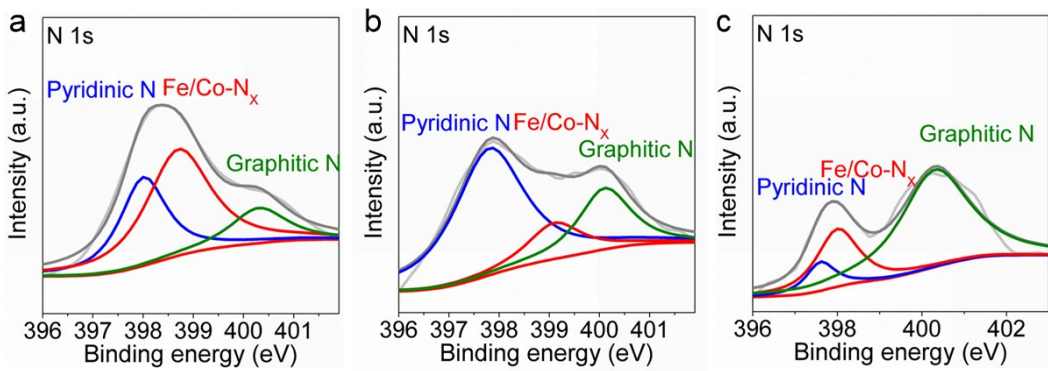


Fig. S11 The high resolution N 1s XPS spectra of FeCo-N-C-600 (a), FeCo-N-C-700 (b), and FeCo-N-C-800 (c).

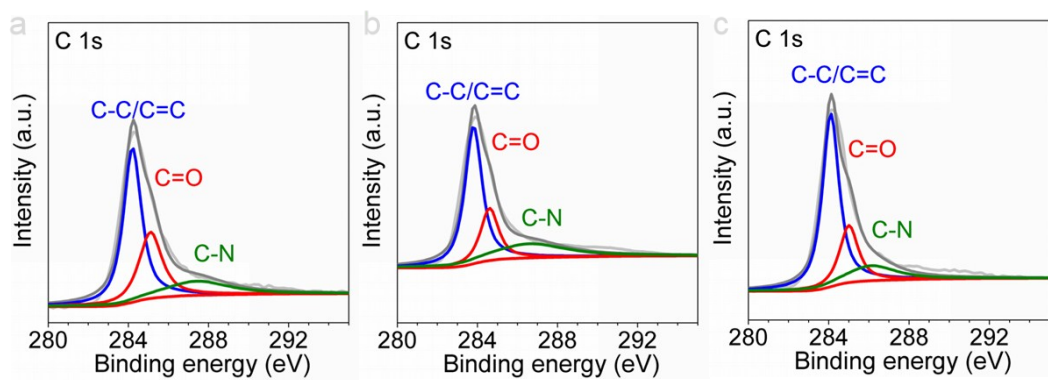


Fig. S12 The high resolution C 1s XPS spectra of FeCo-N-C-600 (a), FeCo-N-C-700 (b), and FeCo-N-C-800 (c).

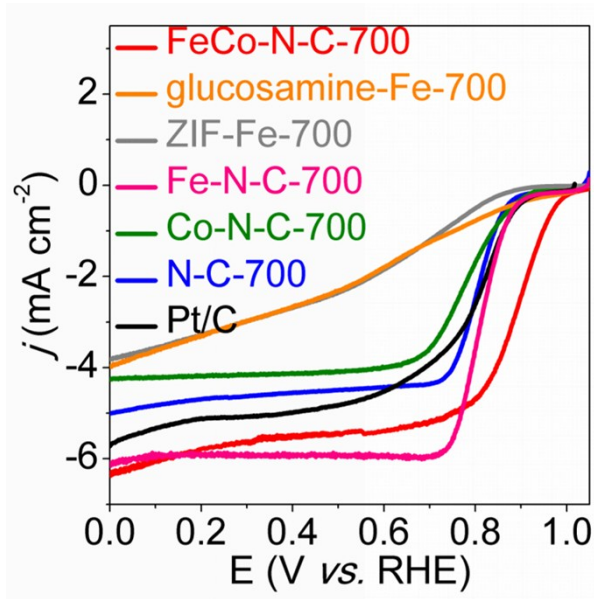


Fig. S13 ORR polarization curves for different catalysts on RDE at 1600 rpm.

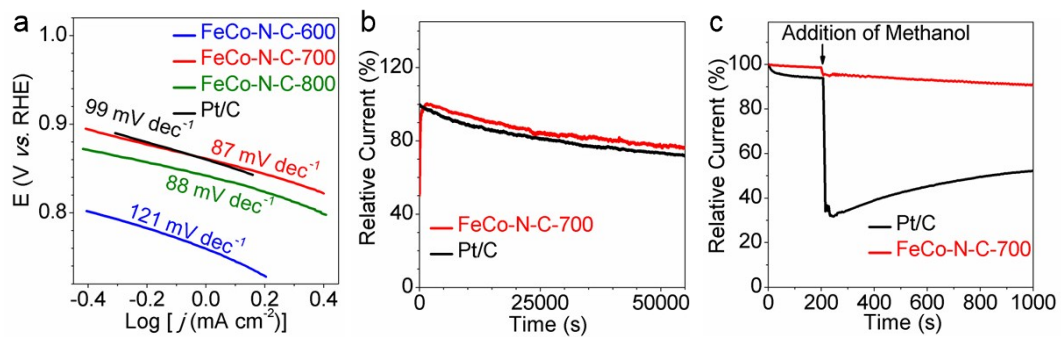


Fig. S14 (a) Tafel slopes of FeCo-N-C-T and Pt/C. (b) Durability evaluation on i-t chronoamperometric responses and (c) methanol effect for ORR at FeCo-N-C-700 and Pt/C.

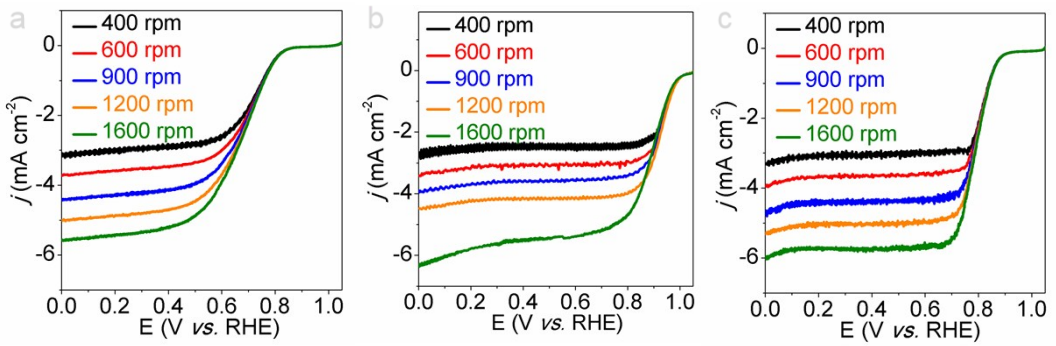


Fig. S15 The ORR polarization curves at different rotating rates of FeCo-N-C-600 (a), FeCo-N-C-700 (b), and FeCo-N-C-800 (c).

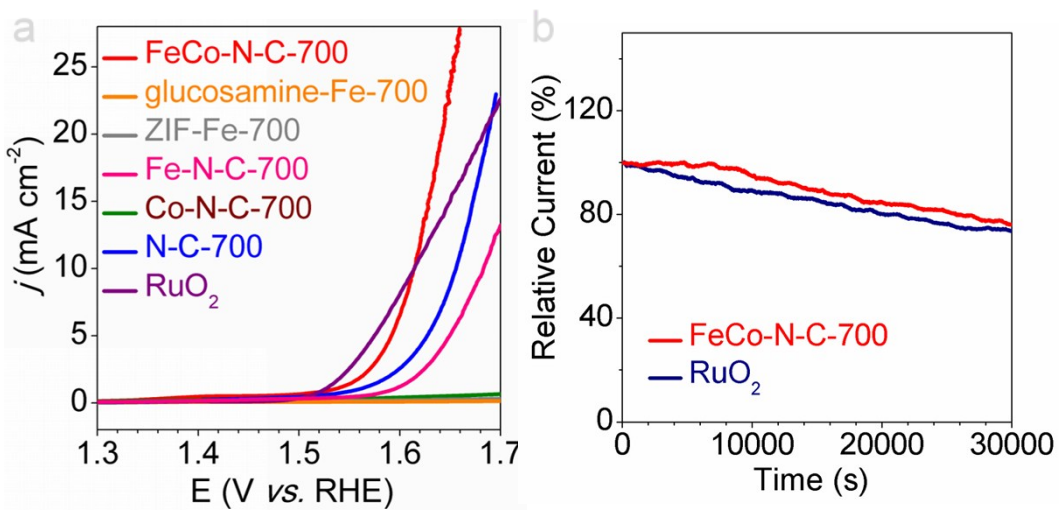


Fig. S16 (a) OER polarization curves for different catalysts on RDE at 1600 rpm. (b) Durability evaluation on i-t chronoamperometric responses for OER at FeCo-N-C-700 and RuO₂.

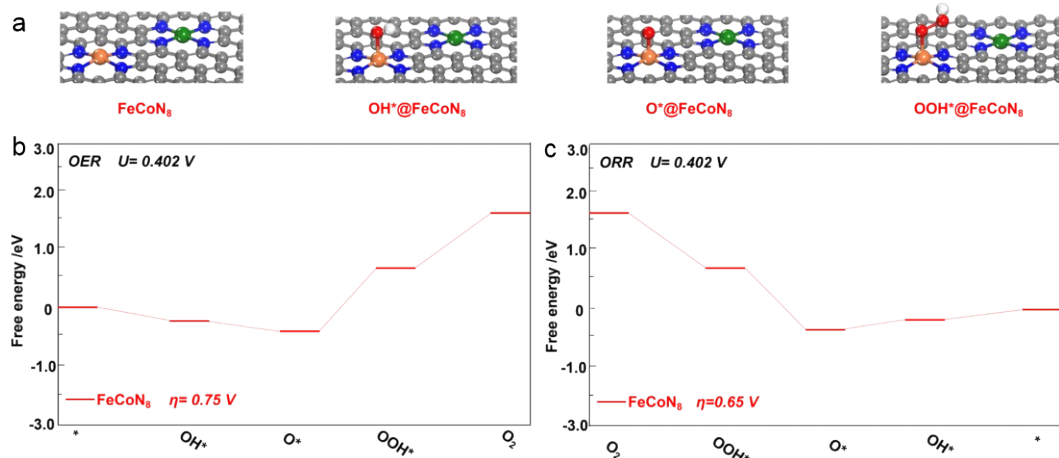


Fig. S17 (a) Schematic of the FeCoN₈ (Fe site), showing the possible positions of dopants. Free energy diagram of FeCoN₈ with the best catalytic performance at the equilibrium potential ($U_0 = 0.402 \text{ V}$) for (b) OER and (c) ORR in alkaline medium.

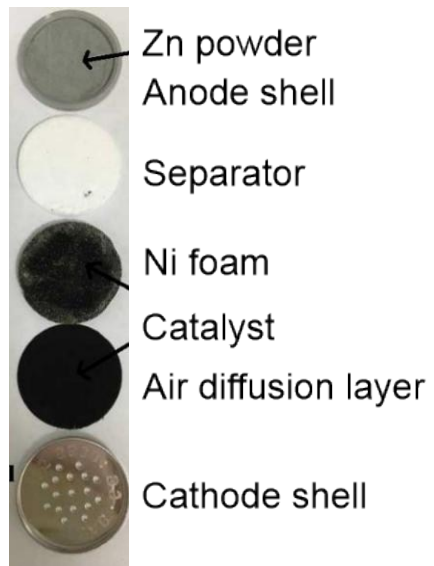


Fig. S18 Digital image of the primary button cell ZAB.

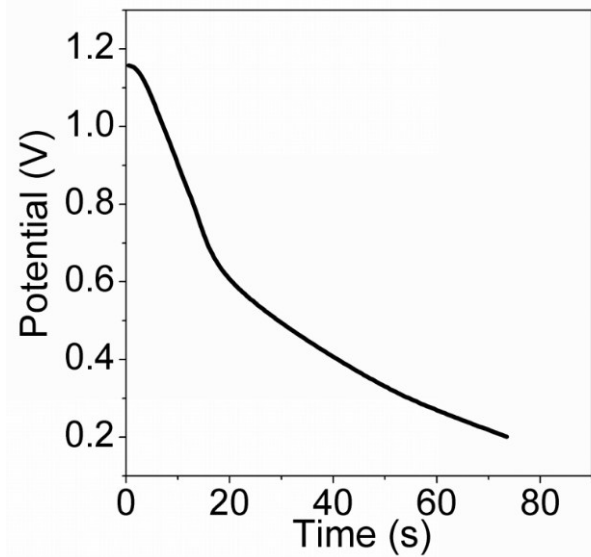


Fig. S19 Discharging curve of the primary ZAB catalyzed by pure Ni foam with an increasing current density of $1 \text{ mA cm}^{-2}/\text{s}$.

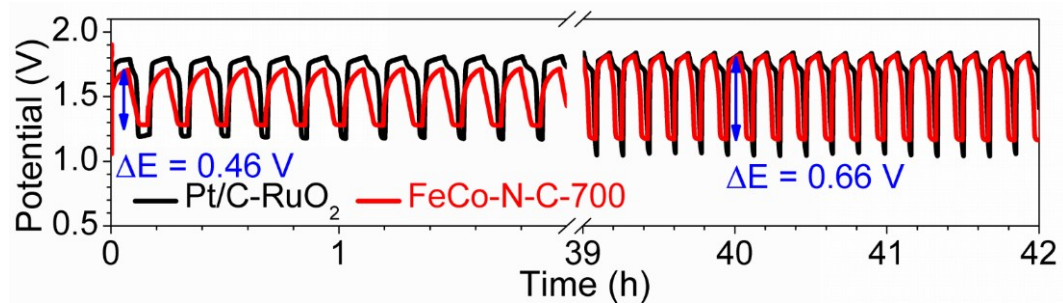


Fig. S20 Discharge/charge cycling curves of Zn–air batteries using FeCo-N-C-700 and Pt/C + RuO₂ for the air electrodes (0.2 mg cm⁻² for ORR and 0.6 mg cm⁻² for OER) at a current density of 5 mA cm⁻².

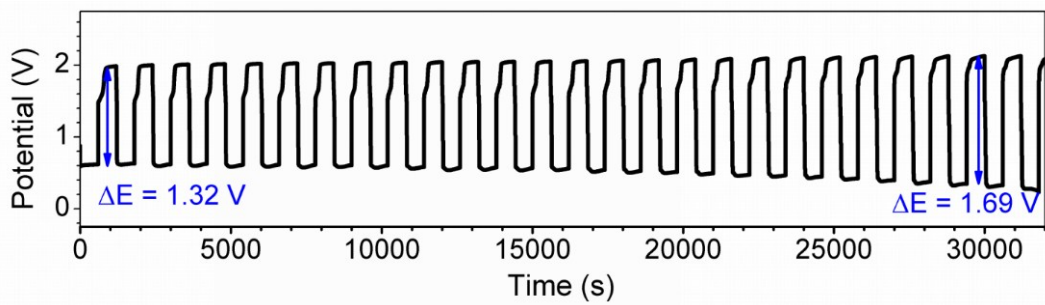


Fig. S21 Discharge/charge cycling curves of all-solid-state Zn–air batteries using FeCo-N-C-700

for the air electrodes at a current density of 0.5 mA cm^{-2} .

Table S1 XPS spectra analysis for FeCo-N-C-T samples.

Sample	C1s (%)	N1s (%)	O1s (%)	Fe2p (%)	Co2p (%)	Zn2p3 (%)
FeCo-N-C-600	76.65	8.69	9.17	1.32	1.89	2.27
FeCo-N-C-700	86.95	3.44	6.46	1.05	1.76	0.34
FeCo-N-C-800	86.59	2.01	8.29	1.16	1.94	0.00

Table S2 XPS spectra analysis for FeCo-N-C-T samples of N 1s signal.

Sample	Pyridinic N	Fe/Co-N _x	Graphitic N
FeCo-N-C-600	398.0 eV, 32.2%	398.7 eV, 52.6%	400.3 eV, 15.2%
FeCo-N-C-700	397.8 eV, 63.3%	399.1 eV, 13.9%	400.1 eV, 22.8%
FeCo-N-C-800	397.6 eV, 8.6%	398.0 eV, 24.6%	400.3 eV, 66.8%

Table S3 Comparison of bifunctional catalytic performance in alkaline solution between FeCo-N-C-700 and other previously reported catalysts.

Catalyst	OER performance		ORR performance		ΔE	Ref.
	Overpotential [mV]	$E_{1/2}$ vs RHE [V]	[V]			
FeCo-N-C-700	370	0.896		0.71	This work	
Co/N-PCC	410	0.838		0.802	1	
CoNC@GF	430	0.87		0.79	2	
Co-NC@ Al ₂ O ₃	417	0.86		0.787	3	
Co-BTC-bipy-700	400	0.79		0.84	4	
Co-N-PHCNTs	390	0.89		0.73	5	
Co SA@NCF/CNF	400	0.88		0.75	6	
FeN _x -PNC	395	0.86		0.775	7	

Table S4 The ΔE_{ads} and ΔG_{ads} of oxygenated intermediates involved in OER and ORR processes on Fe(Co)N₄ or FeCoN₈.

Intermediates	FeN ₄ (eV)	CoN ₄ (eV)	(Co site)	(Fe site)
			FeCoN ₈ (eV)	FeCoN ₈ (eV)
ΔE_{OH^*}	0.68	0.82	0.73	0.54
ΔG_{OH^*}	0.72	0.86	0.77	0.58
ΔE_{O^*}	1.37	3.21	2.16	1.26
ΔG_{O^*}	1.33	3.16	2.12	1.22
ΔE_{OOH^*}	3.66	3.79	3.32	3.19
ΔG_{OOH^*}	3.67	3.80	3.33	3.20

Table S5 The ΔG of various reactions and η for the OER and ORR processes over Fe(Co)N₄ or FeCoN₈.

Reactions	ΔG (eV)	η (V) (eV)	ΔG (eV)	η (V) (eV)	ΔG (eV)	η (V) (eV)	ΔG (eV)	η (V) (eV)
FeN ₄		CoN ₄		(Co site)		(Fe site)		
	(eV)	(eV)					FeCoN ₈ (eV)	FeCoN ₈ (eV)
OH ⁻ * → OH* + e ⁻	-0.11	$\eta^{\text{OER}} =$ 0.04	$\eta^{\text{OER}} =$ 0.06	$\eta^{\text{OER}} =$ -0.06	$\eta^{\text{OER}} =$ -0.25	$\eta^{\text{OER}} =$ 0.75		
OH ⁻	-0.22	1.11	1.47	1.07	0.52	0.36	-0.19	
+ OH* → O* + H ₂ O		$\eta^{\text{ORR}} =$ 0.62		$\eta^{\text{ORR}} =$ 0.60		$\eta^{\text{ORR}} =$ 0.46		$\eta^{\text{ORR}} =$ 0.65
+ e ⁻								
OH ⁻	1.51		-0.20		0.38		1.15	
+ O* → OOH* + e ⁻								
OH ⁻	0.42		0.29		0.76		0.89	
+ OOH* → * + O ₂ +								
H ₂ O + e ⁻								

Table S6 The Peak power density of recently reported bifunctional electrocatalysts.

Air catalysts	Current density (mA cm ⁻²)	Peak power density (mW cm ⁻²)	Ref.
FeCo-N-C-700	240	150	This work
Co-N-CNTs	90	101	8
Co/N-PCC	180	127.86	1
Co-NC@ Al ₂ O ₃	90	72.4	3
MnO@Co-N/C	225	130.3	9
C-MOF-C2-900	120	105	10
Co-N-PHCNTs	130	125.41	5
Co@Co ₃ O ₄ @NC-900	60	64	11

Table S7 The rechargeable ZAB performance of recently reported bifunctional ORR/OER electrocatalysts.

Air catalysts	Current density (mA cm ⁻²)	Number of cycle	Voltage gap (V)	Ref.
FeCo-N-C-700	1	360	0.52	This work
FeCo-N-C-700	5	240	0.66	This work
Co-N-CNTs	2	130	/	8
Co/N-PCC	5	40	1.05	1
Co@Co ₃ O ₄ @NC-900	5	100	0.66	11
CoNiFe-S MNs	2	120	0.74	12
CoP@mNSP-C	10	180	0.86	13
Co-N,B-CSs	5	128	1.35	14
S,N-Fe/N/C-CNT	5	100	1	15
Co ₃ O ₄ -NP/N-rGO	5	118	0.87	16

Reference

1. Q. X. Luo, L. P. Guo, S. Y. Yao, J. Bao, Z. T. Liu and Z. W. Liu, *J Catal*, 2019, **369**, 143-156.
2. S. S. Liu, M. F. Wang, X. Y. Sun, N. Xu, J. Liu, Y. Z. Wang, T. Qian and C. L. Yan, *Adv. Mater.*, 2018, **30**, 1704898.
3. L. Zhu, D. Z. Zheng, Z. F. Wang, X. S. Zheng, P. P. Fang, J. F. Zhu, M. H. Yu, Y. X. Tong and X. H. Lu, *Adv. Mater.*, 2018, **30**, 1805268.
4. X. P. Sun, S. X. Sun, S. Q. Gu, Z. F. Liang, J. X. Zhang, Y. Q. Yang, Z. Deng, P. Wei, J. Peng, Y. Xu, C. Fang, Q. Li, J. T. Han, Z. Jiang and Y. H. Huang, *Nano Energy*, 2019, **61**, 245-250.
5. Y. Guan, Y. L. Li, S. Luo, X. Z. Ren, L. B. Deng, L. N. Sun, H. W. Mi, P. X. Zhang and J. H. Liu, *Applied Catalysis B-Environmental*, 2019, **256**, 117871.
6. D. X. Ji, L. Fan, L. L. Li, S. J. Peng, D. S. Yu, J. N. Song, S. Ramakrishna and S. J. Guo, *Adv. Mater.*, 2019, **31**, 1808267.
7. L. T. Ma, S. M. Chen, Z. X. Pei, Y. Huang, G. J. Liang, F. N. Mo, Q. Yang, J. Su, Y. H. Gao, J. A. Zapien and C. Y. Zhi, *Acs Nano*, 2018, **12**, 1949-1958.
8. T. T. Wang, Z. K. Kou, S. C. Mu, J. P. Liu, D. P. He, I. S. Amiinu, W. Meng, K. Zhou, Z. X. Luo, S. Chaemchuen and F. Verpoort, *Adv Funct Mater*, 2018, **28**, 1705048.
9. Y. N. Chen, Y. B. Guo, H. J. Cui, Z. J. Xie, X. Zhang, J. P. Wei and Z. Zhou, *J. Mater. Chem. A*, 2018, **6**, 9716-9722.
10. M. D. Zhang, Q. B. Dai, H. G. Zheng, M. D. Chen and L. M. Dai, *Adv. Mater.*, 2018, **30**, 1705431.

11. Z. Y. Guo, F. M. Wang, Y. Xia, J. L. Li, A. G. Tamirat, Y. R. Liu, L. Wang, Y. G. Wang and Y. Y. Xia, *J. Mater. Chem. A*, 2018, **6**, 1443-1453.
12. H. Z. Yang, B. Wang, H. Y. Li, B. Ni, K. Wang, Q. Zhang and X. Wang, *Adv Energy Mater*, 2018, **8**, 1801839.
13. S. H. Ahn and A. Manthiram, *Small*, 2017, **13**, 1702068.
14. Y. Y. Guo, P. F. Yuan, J. N. Zhang, Y. F. Hu, I. S. Amiinu, X. Wang, J. G. Zhou, H. C. Xia, Z. B. Song, Q. Xu and S. C. Mu, *Acs Nano*, 2018, **12**, 1894-1901.
15. P. Chen, T. Zhou, L. Xing, K. Xu, Y. Tong, H. Xie, L. Zhang, W. Yan, W. Chu, C. Wu and Y. Xie, *Angew Chem Int Edit*, 2017, **56**, 610-614.
16. Z. Y. Bai, J. M. Heng, Q. Zhang, L. Yang and F. F. Chang, *Adv Energy Mater*, 2018, **8**, 1802390.